Azhar Int J Pharm Med Sci 2025; Vol 5 (2):87- 105
Research Article

Open Acces

Print ISSN: 2735-4598
Online ISSN: 2735-4601

Bis-thiazole Hybrids as Promising Candidates in Controlling Diabetes Mellitus: *in vivo*, *in vitro* Evaluation, in Silico ADMET, and Docking Studies

Aya Thabet [1,*], Moustafa S. Abusaif [2], Yousry A. Ammar [2], Shimaa M. Abd El-Gilil [1], Heba M. A. Elsanhory [3], and Eman A. Fayed [1,*]

[1] Pharmaceutical Organic Chemistry Department, Faculty of Pharmacy (Girls), Al-Azhar University, Cairo 11754, Egypt.
[2] Chemistry Department, Faculty of Science (Boys), Al-Azhar University, Cairo 11884, Egypt.
[3] Pharmacology & Toxicology Department, Faculty of Pharmacy, Sinai University- Kantara Branch, Ismailia, Egypt.

* Correspondence: ayathabetmohammed69@gmail.com, alfayed_e@azhar.edu.eg

Article history: Received 2024-06-14 Revised 2024-08-12 Accepted 2024-09-14

Abstract: The worldwide healthcare systems continue to bear a heavy load from diabetes mellitus (DM) and its associated consequences. Based on this information, our goal was to develop and evaluate novel *bis*-thiazole hybrids **6–8**, which were produced using a structural hybridization technique based on derivatives of thiosemicarbazone and phenacyl bromide. The potential of the new bis-thiazole derivatives to reduce blood glucose levels in normal rats was assessed *in vivo* as part of their antidiabetic activity. They were contrasted with the prescription medication pioglitazone. Sprague-Dawley male rats exposed to compound **7** showed lower blood glucose levels than those exposed to pioglitazone. Additionally, the evaluation focused on compound **7**'s agonist activity on PPAR-γ and its inhibitory effects on *α*-amylase and *α*-glucosidase. Compound **7** inhibited *α*-glucosidase significantly (IC_{50} = 3.708 ± 0.07 mM/mL) compared to ordinary acarbose (IC_{50} = 0.74 ± 0.15 mM/mL). Furthermore, hybrid **7**'s IC_{50} values (84.4±4.19.9) showed limited inhibitory activity against *α*-amylase. Additionally, this molecule's PPAR-*γ* agonist activity was evaluated and shown to be effective. The IC_{50} value was 1.057±0.030 ng/mL, greater than pioglitazone's (1.912±0.11 ng/mL). All available evidence suggests compound 7 may be a viable hybrid for novel anti-diabetic medications that will be more efficient than Pioglitazone and less toxic. Furthermore, i*n silico* ADMET and docking studies were performed.

Keywords: Type-I diabetes; Type-II diabetes; *α*-amylase; *α*-glucosidase; PPAR-*γ;* thiazole; thiosemicarbazone; *bis*-thiazole.

1. INTRODUCTION

Diabetes mellitus is a prevalent metabolic illness worldwide[1]. It is characterized by fasting and postprandial persistent hyperglycemia and is brought on by either Type-I (deficiency in insulin production) or Type-II (cells' inability to react appropriately to normal insulin levels)[2]. Because of obesity brought on by a diet high in energy-dense meals, fast food, and saturated fats, it affects women more frequently than men[3,4]. Pancreatic cell dysfunction or defect in insulin uptakes by the cells are the identifying features that lead to elevated glucose levels in blood [5]. Physical inactivity, high-energy diets, obesity, severe and prolonged stress associated with today's modern life are the main causes of the raising of this syndrome also many drugs can impair insulin action as contraceptive steroids, in addition to Genetic factors [6] It is associated with other destructive health complications such as retinopathy with potential loss of vision, nephropathy leading to renal failure, poor wound healing, peripheral neuropathy with risk of foot ulcers, amputations, sexual dysfunction,

increasing incidence of infection, bone fracture, increased risk of cancer [7] and atherosclerotic cardiovascular diseases [8].

Diabetes is treated with medications that lower blood glucose levels. These drugs are referred to as oral hypoglycemic agents and are taken orally. Diabetes can be managed with the aid of many kinds of these medications. For instance, glinides and sulfonylureas are examples of insulin secretagogues that increase pancreatic insulin secretion[9]. But one of these medications' most frequent adverse effects is hypoglycemia[10].

Conversely, the enzymes α-amylase and α-glucosidase transform oligosaccharides and disaccharides into monosaccharides. When these enzymes are inhibited, the rise in blood glucose levels following carbohydrate consumption can be delayed and lessened[11]. Acarbose is a medication that is frequently used to block these enzymes, although it can have negative side effects that include flatulence, diarrhea, and soreness in the abdomen[12]. Insulin sensitizers increase peripheral glucose absorption and insulin sensitivity, which is important for controlling diabetes mellitus. They work by stimulating the peroxisome proliferator-activated receptor (PPAR-γ), just like thiazolidinediones (TZD). As a result of this activation, the glucose transporters GLUT1 and GLUT4 are expressed more often and translocate to the cell surface[9], increasing the absorption of glucose by adipocytes and muscle cells and lowering plasma levels of glucose. Since adipose tissue is where PPAR-γ is mainly expressed, it is a crucial target for the control of diabetes[10].

Since diabetes complications are linked to both immediate and long-term healthcare costs, targeting the enzymes or receptors involved in the absorption and metabolism of glucose and other carbohydrates that elevate postprandial glucose levels remains an appealing and successful strategy for drug discovery and the development of new anti-diabetic agents with low side effects, high efficacy, and low cost [13].

Heterocyclic compounds, specifically thiazole derivatives, exhibit various biological properties such as antimicrobial, antifungal, anti-inflammatory, antidepressant, antipsychotic, antipyretic[14] and antidiabetic activities[15]

The thiazole scaffold is a prevalent and versatile structure found in numerous pharmaceutical compounds. It exhibits a diverse range of pharmaceutical activities and possesses several reactive sites, which expand its applications and offer novel solutions for challenges in medicinal and synthetic chemistry[16]. Thiazole nucleus presents in many natural products like penicillin as anti-biotic, vitamin B1, and anti-cancer drug epothilone, in addition, many marketing drugs as sulfa-drug (sulfathiazole), anti-cancer drug (tiazofurin) and non-steroidal anti-inflammatory drug (meloxicam) .Compounds containing more than thiazole nucleus also have good pharmacological properties as anti-cancer, anti-bacterial, skin treatment.[17]

Thiosemicarbazones (TSCs) have been gaining significant attention in the field of medicinal chemistry for their favorable biological activities. The reason behind their efficacy is often attributed to their ability to sense ions and form bonds with metal ions owing to their diverse bonding modes[18].

The most used thiazolidinediones are synthetic antidiabetic TZD, such as pioglitazone (ACTOS®) and rosiglitazone (Avandia®), which were approved by the FDA in 2000 [19]. Because rosiglitazone may cause fluid retention-related heart failure, its use is rather limited. Pioglitazone also causes urothelial bladder tumours[20], beginning from this point the whole world is in great demand for developing new anti-diabetic medication with high efficacy and low toxicity.

The present investigation aims to create and produce novel *bis*-thiazole configurations and explore their *in vivo* hypoglycemic impact. Subsequently, the potential compounds were examined in *vitro* as inhibitors of α-amylase, α-glucosidase, and as a PPAR-γ agonist. Docking studies verified the outcomes of the biologicalassessments. The novel compounds' physicochemical characteristics, drug-likeness, pharmacokinetics properties, and toxicity were assessed using *in silico* methods. Lately, thiazole has drawn more interest because of its possible application as a diabetes management drug; pioglitazone is one such example [10]. According to a paper, substance (A) increased PPAR-γ gene expression 2.10 times more than standard medications pioglitazone (1.5 times) and rosiglitazone (1.0 times) [21]. Compound (B) has noteworthy inhibitory ability against both α-glucosidase and α-amylase [22]. figure 1.

Our study showed the synthetic pathway and hypoglycemic activity of *bis* thiazole derivatives which displayed more strong activity toward Peroxisome Proliferator-Activated Receptor (PPAR-γ) than the standard drug used (pioglitazone)

with low toxicity, The IC_{50} value was 1.057±0.030 ng/mL for compound 7, greater than pioglitazone's (1.912±0.11 ng/mL).

While the same compound showed good alpha-glucosidase inhibitory activity with an IC_{50} value of 3.708± 0.07 mM/mL, when compared with standard drug acarbose 0.74 ± 0.15 mM/mL

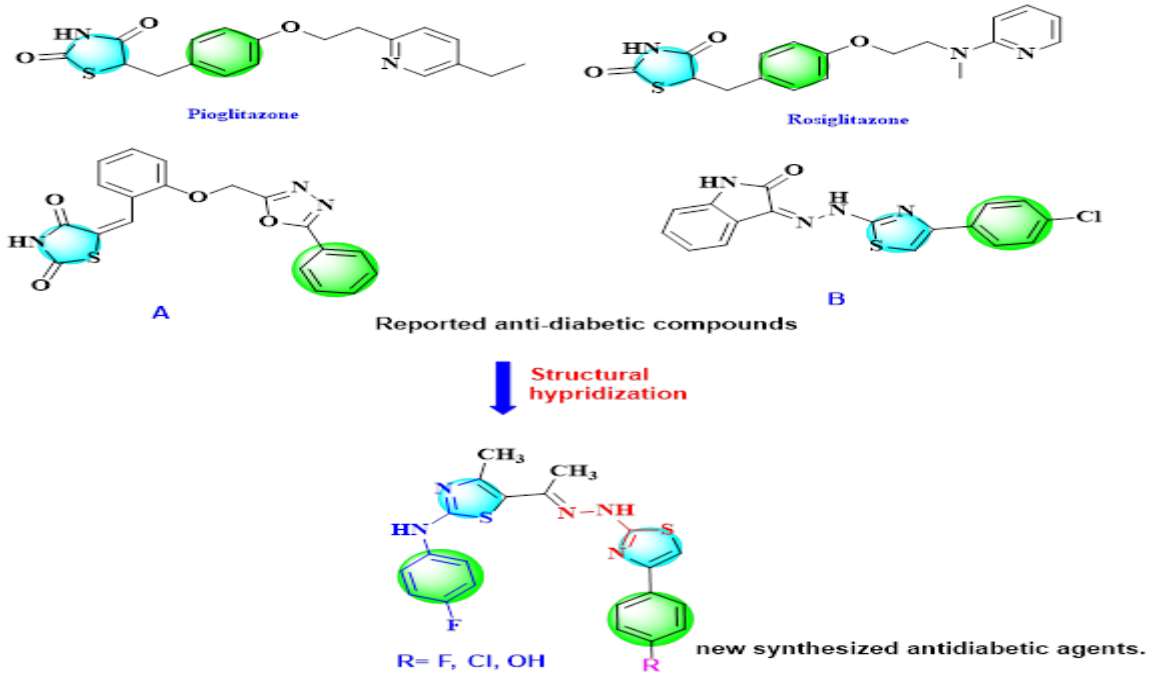

Figure 1. rational study of the new synthesized compounds.

2. METHODS

2.1. Chemistry

2.1.1. Materials and Physical Measurements

All materials procured from commercial sources were utilized without undergoing any additional purification processes. The verification of the purity of the synthesized compounds and the progress of the reaction was conducted through the application of ascending thin-layer chromatography (TLC). For the visualization of the TLC spots, the aid of a UV lamp and an iodine chamber were employed. The determination of the melting points was accomplished using the Open Capillary Method and a Programmable Digital Melting Point Apparatus, with the possibility of the measurements being uncorrected. The analysis of the IR spectra was performed utilizing the KBr disk technique on a Nicolet IR 200 FT-IR Spectrophotometer (vmax in cm^{-1}) at the Pharmaceutical Analytical Unit, Faculty of Pharmacy, Al-Azhar University, Egypt. The Gemini 400/500 MHz and Mercury 101/125 MHz NMR Spectrometers were used to record the Nuclear Magnetic Resonance (NMR) spectra, more especially the ^{1}H and ^{13}C NMR spectra. These tests were carried out in Cairo, Egypt, at the Ministry of Defense's Main Chemical Warfare Laboratories, Chemical Warfare Department. The Mansoura University Faculty of Science additionally contributed to this study. Parts per million (ppm) was the unit of measurement for the chemical shifts, and DMSO-d6 was used as the solvent. TMS was used as an internal reference. On the other side, a Shimadzu GC/MS-QP5050A Spectrometer's DI-50 unit was used to acquire the mass spectrum at 70 electron volts (eV). The Regional Centre for Mycology and Biotechnology (RCMB) at Al-Azhar University served as the site of this experiment. Relative abundance (%) is expressed as *m/z* (formula) in the mass spectrum. Moreover, the Regional Centre for Mycology and Biotechnology carried out an elemental analysis involving Carbon (C), Hydrogen (H), and Nitrogen (N). Unless otherwise noted, there was no more than ± 0.4% deviation between the obtained values and the theoretical values when compared. Finally, it's critical to remember that the terms "s," "d," "t," and "m" stand for the singlet, doublet, triplet, and multiplet, respectively.

2.1.2. Synthesis of Organic Materials

2.1.2.1. Synthesis of 1-(2-((4-fluorophenyl) amino)-4-methyl thiazole-5-yl) ethan-1-one (3)

According to the literature survey [23], compound 1-(2-((4-fluorophenyl) amino)-4-methyl

thiazole-5-yl) ethan-1-one was synthesized as pure grayish powder solid with M.P.: 150 −152 ℃.

2.1.2.2. Synthesis of 2-(1-(2-((4-fluorophenyl)amino)-4-methylthiazol-5-yl)ethylidene)hydrazine -1-carbothioamide (4)

For 4 hours, a mixture of compound **1** (0.01 mol) and hydrazine carbothioamide (0.01 mol) was heated under reflux in absolute ethanol (20 mL) with acetic acid (0.5 mL) as the catalyst. The reaction mixture was left at room temperature for 5 hours with no interruptions. The solid product was then filtered and crystallized from ethanol.

Yield: (75%); orange powder; **M.P**.:154-155ºC; **IR** (υ /cm^{-1})= 3436 (NH), 3160 (br.NH_2), 3059(CH-arom), 2947(CH-aliph) 1625 (C=N); **^{1}HNMR** (500 MHz, DMSO-d_6): *δ (ppm)* = 1.86, 2.37 (6H, s, $2CH_3$), 7.16 (2H, d, Ar-H, *J* = 8.5 Hz), 7.58 (2H, d, Ar-H, *J* = 9.0 Hz), 10.31 (2H, s, NH_2, D_2O exchangeable), 9.11, 9.66, (2H, s, 2NH, D_2O exchangeable); **^{13}CNMR** (126 MHz, DMSO-d_6): *δ (ppm)* = 17.40, 18.95 ($2CH_3$), 116.20, 116.38, 122.81, 137.01, 149.22, 157.13, 162.26, 159.16 (C=N), 182.30 (C=S); **MS** (*m/z*): 323.47 (M.+, 19.44%), 92.28 (100%); **Anal. Calc.** for $C_{13}H_{14}FN_5S_2$ (323.41) C, 48.28; H, 4.36; N, 21.66; **Found:** C, 48.22; H, 4.31; N, 21.63.

2.1.2.3. Synthesis of *bis*-thiazole derivatives 6-8

Triethylamine was used as a catalyst in a solution comprising thiosemicarbazone derivative **2** (0.01 mol) and 4-fluoro, 4-chloro, or 4-hydroxy phenacyl bromide (0.01 mol) in 20 mL 100% ethanol. After that, the mixture was heated under reflux for 3 hours. After the reaction was finished (as seen by TLC), the mixture was allowed to come to room temperature before being added to ice-cooled water. Filtration was used to gather the resultant solid, which was then recrystallized in the suitable solvent.

2.1.2.4. *N*-(4-Fluorophenyl)-5-(1-(2-(4-(4-fluorophenyl) thiazol-2-yl)hydrazono)ethyl)-4-methyl-thiazol-2-amine (6)

Yield: (85%); green powder from ethanol; **M.P**.: 130-131ºC. **IR** (υ/ cm^{-1}) = 3328 (NH), 3085 (CH-arom), 2921 (CH-aliph.), 1613 (C=N); **^{1}HNMR** (500 MHz, DMSO-d_6): *δ (ppm)* =2.27, 2.41 (6H, s, $2CH_3$), 7.10 (2H, d, Ar-H, *J* = 9.0 Hz), 7.15 (1H, s, thiazole-H), 7.19 (2H, d, Ar-H, *J* = 9.0 Hz), 7.60 (2H, d, Ar-H, *J* = 9.0 Hz), 7.83 (2H, d, Ar-H, *J* = 8.0 Hz), 10.24, 11.13 (2H, s, 2NH, D_2O exchangeable); **^{13}CNMR** (126 MHz, DMSO-d_6): *δ (ppm)*=17.20, 18.85 ($2CH_3$), 103.98, 116.17, 119.28, 120.41, 127.94, 133.53, 137.02, 137.82, 147.19, 157.24, 158.48, 161.11, 161.79, 170.12 (Ar-Cs),156.55 (C=N); **MS** (*m/z*): 441.60 ($M^{\cdot+}$, 18.87%), 114.29 (100%); **Anal. Calc.** for $C_{21}H_{17}F_2N_5S_2$ (441.52) C, 57.13; H, 3.88; N, 15.86; **Found**: C, 57.16; H, 3.81; N, 15.90.

2.1.2.5. 5-(1-(2-(4-(4-Chlorophenyl)thiazol-2-yl) hydrazono)ethyl)-*N*-(4-fluorophenyl)-4-methyl-thiazol-2-amine (7)

Yield: (92%); grayish powder from ethanol; **M.P**.:137-138ºC. **IR** (υ/ cm^{-1}) = 3310 (NH), 3064 (CH -arom.), 2925 (CH- aliph.), 1615 (C=N); **^{1}HNMR** (400 MHz, DMSO-d_6): *δ (ppm)*= 2.33, 2.43 (6H, s, $2CH_3$), 7.15 (2H, d, Ar, *J* = 8.4 Hz), 7.32 (1H, s, thiazole-H), 7.37 (2H, d, Ar, *J* = 8.4 Hz), 7.55 (2H, d, Ar, *J* = 8.0 Hz), 7.61 (2H, d, Ar, *J* = 9.6 Hz), 10.30, 11.46 (2H, s, 2NH, D_2O exchangeable); **^{13}CNMR** (101 MHz, DMSO-d_6): *δ (ppm)*=18.95, 30.18 ($2CH_3$), 103.29, 116.11, 120.38, 128.83, 129.68, 131.60, 132.88, 134.11, 136.22, 147.74, 157.17, 159.43, 161.78, 165.68 (Ar-Cs), 156.32 (C=N); **MS** (*m/z*): 459.95 (M^{+2}, 30.10%), 457.63 ($M^{\cdot+}$, 28.87%), 309.08 (100%); **Anal. Calc.** for $C_{21}H_{17}ClFN_5S_2$ (457.97) C, 55.08; H, 3.74; N, 15.29; **Found**: C, 55.01; H, 3.68; N, 15.21.

2.1.2.6. 4-(2-(2-(1-(2-((4-Fluorophenyl)amino)-4-methylthiazol-5-yl)ethylidene)hydrazinyl)-thiazol-4-yl)phenol (8)

Yield: (50%); green powder from ethanol; **M.P**.: 129-130ºC. **IR** (υ/cm^{-1}) = 3200 (NH), 3250 (OH), 3070 (CH-arom), 2924(CH-aliph), 1606 (C=N); **^{1}HNMR** (400 MHz, DMSO-d_6): *δ (ppm)*=2.32, 2.51(6H, s, $2CH_3$), 6.70 (2H, d, Ar-H, *J* = 8.0 Hz), 6.98 (1H, s, thiazole-H), 7.14 (2H, d, Ar-H, *J* = 8.4 Hz,), 7.21 (2H, d, Ar-H, *J* = 10.8 Hz), 7.64(2H, d, Ar-H, *J* = 6.8 Hz.), 9.63, 10.22 (2H, s, 2NH, D_2O exchangeable), 11.31 (1H, s, OH, D_2O exchangeable); **^{13}CNMR** (101 MHz, DMSO-d_6): *δ (ppm)* =18.95, 30.32 ($2CH_3$), 103.86, 116.00, 116.45, 119.16, 120.40, 129.41, 133.74, 137.68, 149.63, 156.44, 157.67, 158.68,171.86 (Ar-Cs), 154.03 (C=N), 161.66 (C-OH); **MS** (*m/z*): 439.26 ($M^{\cdot+}$, 26.27%), 198.35 (100%). **Anal. Calc.** for $C_{21}H_{18}FN_5OS_2$ (439.53) C, 57.39; H, 4.13; N, 15.93; **Found**: C, 57.32; H, 4.09; N, 15.95.

2.2. Biological Activity Study

2.2.1. Hypoglycemic Evaluation of the New Synthesized Compounds 6-8

2.2.1.1. Experimental design

To reduce variability and achieve more consistent blood glucose readings in the animals, all produced compounds were tested *in vivo* on rats who had fasted for 14-18 hours the night before [24]. The experiment had five groups of six normal fasting rats, randomized at random. As a negative control, two groups were given a solution of 1% carboxymethyl cellulose (CMC) in water, while a positive control group received an oral dose of 30 mg/kg of pioglitazone dissolved in CMC. Each of the

remaining groups (3–5) received one of the tested compounds at a dose of 30 mg/kg dissolved in CMC[19]. After 30 minutes of administering each test chemical, each animal received an oral glucose solution of 2.5 g/kg[25].

2.2.1.2. Animals

The examination was carried out on male Sprague-Dawley rats obtained from Nile Pharmaceuticals Company, Cairo, Egypt. The rats were allowed to adapt to the laboratory environment for one week before the experiment. They were housed in standard stainless-steel cages under controlled experimental conditions which included a temperature of 25 ± 2°C, relative humidity of 55 ± 10%, and a light-dark cycle of 12 hours. The rats were provided with standard diet pellets and water was given ad libitum. The research was conducted in adherence to the ethical guidelines set by the Faculty of Pharmacy at Al-Azhar University, Egypt ethical approval number (405). The handling of the animals followed the guidelines outlined in the publication titled "Guide for Care and Use of Laboratory Animals" (NIH Publication No. 85-23, revised 2011).

2.2.1.3. Gathering of blood samples and determination of blood glucose levels

Samples were obtained *via* the tail vein using excision, and blood glucose levels were assessed at 30-minute and one-hour intervals after the administration of glucose, for each animal. using a one-touch glucometer (ACCU-CHEK® INSTANT System Roche Diabetes Care Limited Charles Avenue, Burgess Hill RH15 9RY, UK) [26].

2.2.1.4. Statistical analysis

SEM, or standard error of the mean, was used to present the data. For statistical comparisons, Tukey's multiple comparison test was performed after a one-way ANOVA. At the $P<0.05$ significant threshold, the values were deemed statistically significant [25].

2.2.2. In-vitro α-Amylase Inhibition Assay

2.2.2.1. Principle

Using the 100 assays in the *α*-Amylase Inhibitor Screening Kit 2/19 Catalogue # K482-100, a series of kinetic studies were carried out to clarify the mechanism of enzyme inhibition. The 96-well microplate assay for exploring potential α-amylase inhibitors is simple and consistent with the help of Bio Vision's α-Amylase Inhibitor Screening kit. The chromophore (pNP; OD = 405 nm) is formed into smaller fragments by the hydrolysis of the synthetic substrate by the human α-amylase enzyme in this kit. Furthermore, the kit includes a strong and targeted inhibitor.

To investigate the inhibition activity, various concentrations of *α*-amylase inhibitors were employed alongside different concentrations of the inhibitor substrate (*p*-nitrophenyl R-D-maltoside (NPM)) within the reaction mixture.

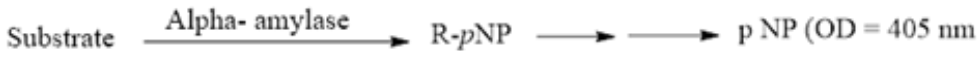

2.2.2.2. Measurement

Determine the optical density at a wavelength of 405 nm using a kinetic approach over a period of 20 to 25 minutes at ambient temperature. select two-time points (t1 and t2) within the linear region of the graph and acquire the corresponding absorbance values (OD1 and OD2) utilizing an ELISA reader.

2.2.2.3. Calculation

For each Test Sample [S], Enzyme Control [EC], and Solvent Control [SC], the reading for Background Control [BC] is subtracted. By dividing the change in optical density (OD2 - OD1) by the change in time (t2 - t1), one may find the slope of each well. If [SC] slope is significantly different from [EC], use [SC] readings to determine the suppressive effect of the substance(s) under investigation.

% Relative Inhibition = Slope [EC]−Slope of [S]/ slope of [EC] X100

% Relative Activity = Slope of [S]/Slope of [EC] X100

The IC_{50} values were established by plotting the percentage of inhibition against the logarithm of inhibitor concentration and were computed through non-linear regression analysis based on the average inhibitory measurements. Acarbose was employed as the alpha-amylase inhibitor of reference. The IC_{50} values were designated as the concentration of inhibitor at which 50% of enzyme activity inhibition is observed [27].

2.2.3. Alpha-Glucosidase Assay

2.2.3.1. Principle

Bio Vision's *α*-Glucosidase Inhibitor Screening Kit 06/18 (Catalog # K938-100) examines potential inhibitors of this enzyme. The kit operates by employing the capacity of an active *α*-glucosidase to break down a synthetic substrate, thereby releasing a chromophore with an optical density of 410 nm.

When a glucosidase-specific inhibitor is present, the enzymatic activity is significantly diminished, which can be identified through a reduction in absorbance readings. This assay kit offers a swift, straightforward, and dependable method for conducting high-throughput screening of *α*-glucosidase inhibitors.

2.2.3.2. Measurement

Measure the absorbance rapidly at an optical density of 410 nm in kinetic mode for 60 minutes at room temperature. Select two specific time points (t1 and t2) within the linear range of the graph and acquire the corresponding absorbance values (OD1 and OD2).

2.2.3.3. Calculation

Divide the net change in optical density (A2-A1) values by the change in time (t2-t1) to determine the gradient for each test sample [S], Enzyme Control [EC], Solvent Control [SC], and Background Control [BC]. Deduct the Background Control gradient from [S], [EC], and [SC]. Use the values of [SC] to ascertain the impact of the tested substance if the gradient of [SC] differs noticeably from that of [EC].

% Relative Inhibition = Slope [EC]−Slope of [S]/ Slope of [EC] X100

% Relative Activity = Slope of [S] /Slope of [EC] X100

2.2.3.4. Statistical analysis

The statistical analysis was conducted using Graph Pad Prism version 8.0 for Windows. The values are presented as the mean (±SD), and the comparison between groups was assessed using a one-way analysis of variance (ANOVA). The IC_{50} is determined by employing linear regression to plot the x-y data and fitting it with a linear line.

2.2.4. Determination of Peroxisome Proliferator-Activated Receptor γ [PPAR-γ] Agonist Activity

2.2.4.1. Principle

The Bioscience Human PPAR-γ (Peroxisome Proliferator-Activated Receptor Gamma) ELISA Kit (Catalogue No: MBS2503174 96T) follows the Sandwich-ELISA concept. This kit includes a micro-ELISA plate pre-coated with an antibody targeting Human PPAR-γ. The micro-ELISA plate wells are used to inject the standards or samples, which are subsequently mixed with the appropriate antibody. A biotinylated antibody that recognizes human PPAR-*γ* and an Avidin-Horseradish Peroxidase (HRP) combination are then added to each microplate well and incubated. Free components are removed by washing them away. In each well, the substrate solution is added. The only wells that will turn blue are those that have the biotinylated detection antibody, the Avidin-HRP conjugate, and human PPAR-γ. When a stop solution is added, the enzyme-substrate reaction is halted and the color changes to yellow. Spectrophotometry is used to measure the optical density (OD) quantitatively at a wavelength of 450 nm + 2 nm. The relationship between the concentration of human PPAR-*γ* and the value of OD is direct. By comparing the optical density (OD) of the samples to the standard curve, one can ascertain the concentration of human PPAR-*γ* in the samples.

2.2.4.2. Statistical analysis

The statistical analysis was conducted utilizing Graph Pad Prism version 8.0 for the Windows operating system. The values were expressed as the mean (±SD), and the distinction between groups was evaluated through the implementation of a one-way analysis of variance (ANOVA). The IC_{50} was determined by employing linear regression, where x-y was plotted, and the data was fitted with a linear model.

2.3. *In-silico* Studies

2.3.1. In-silico Physicochemical and ADME Properties Study

Using the interface of the Swiss ADME website (http://www.sib.swiss), all synthesized compounds in the current experiment were screened, together with the standard reference medicines pioglitazone and acarbose [29]. *In silico* ADME characteristics and drug-likeliness prediction were carried out. Chemdraw 19.0 was used to translate the molecular structures into the SMILES database. The resultant SMILES were then entered into the Swiss ADME website to ascertain a number of factors, such as medicinal chemistry friendliness, physicochemical descriptors, pharmacokinetics qualities, and lipophilicity [30–34].

2.3.2. Docking Studies

RCSB PDB (https://www.rscb.org) was used to download the crystal structures 3D of *α*-glucosidase in complex with Acarbose (PDB ID: 5NN8, resolution: 2.45 Å) [35], *α*-amylase in complex with Acarbose (PDB ID: 1B2Y, resolution: 3.20 Å)[36], as well as Peroxisome proliferator Activating Receptor-*γ* (PPAR-*γ)* in complex with Pioglitazone (PDB ID: 5Y2O, resolution: 1.80 Å)[37]. The pdb format was utilized for the purposes of this docking study. To import the protein crystal structure, the Molecular Operating Environment (MOE 2014.09) (Montreal, QC, Canada) was employed[38].The forcefield was configured to MMFF94x. The QuickPrep feature was implemented to eliminate distant water molecules, remedy structural errors, introduce missing hydrogen atoms, compute partial charges, and conduct energy minimization using the default RMS gradient of 0.1 kcal/mol/A. The binding pocket was established. The software ChemBioDraw Ultra 12.0 was employed to depict the structures of the most potent newly synthesized compounds. These structures were subsequently saved in the mol file format and imported into a database in the mdb format. Prior to import, the Wash feature was utilized to rectify any structural errors and incorporate missing hydrogen atoms. Subsequently, partial charges were computed. The appropriate tautomeric states for each compound were carefully chosen and reintroduced into the database. Finally, energy minimization was performed.

The validity of the docking protocol for each protein target was assessed through self-docking of the co-crystallized ligand within the protein's binding site, thereby substantiating the accuracy of the employed docking protocol in this simulation. The verification of the self-docking procedure was confirmed by the minimal RMSD value between the re-docked pose and the co-crystallized ligand, in conjunction with a low energy score (S). Furthermore, the re-docked pose demonstrated the capability to align with the native ligand and occupy critical interactions established by the co-crystallized ligand with the active site hot spots, Figure 3.

An energy score (S) of -19.54 kCal/mol and an RMSD value of 0.5693 were obtained from the docking of acarbose in *α*-glucosidase. Similarly, an energy score (S) of -9.54 kCal/mol and an RMSD value of 0.6385 were obtained upon docking Acarbose in *α*-amylase. Additionally, pioglitazone's docking in PPAR-*γ* produced an energy score (S) of -12.77 kCal/mol and an RMSD value of 0.3703. Table 6 lists the important interactions that occur between each ligand and its corresponding protein.

3. RESULTS and DISCUSSION

3.1. Chemistry.

Plan 1 depicted synthesis of starting material **3** in accordance with known methods [39, 40]. The mechanism of ring closure was also explained in **scheme 2** through Hantsch's method [41], based on the idea that thiosemcarbazone derivatives were a very useful reagent as synthetic starting material for synthesis of thiazoles. This was achieved by ring closure of the derivative of thiourea **1** with 3-chloropentane-2,4-dione (**2**)[42,43].

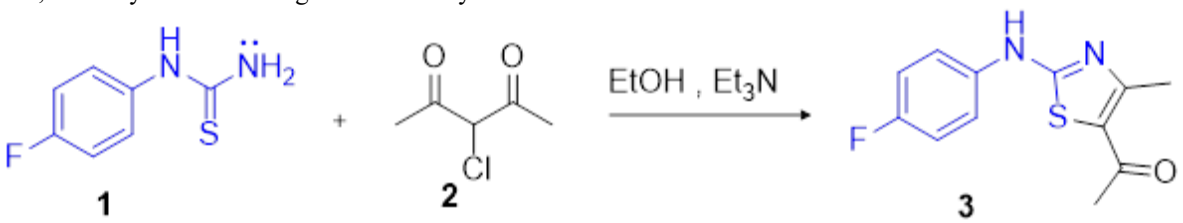

Scheme 1. Synthesis of a1-(2-((4-fluorophenyl)amino).-4-methyl thiazole-5-yl)ethan-1-one (3).

We depend in our work on the synthesis of thiosemicarbazone derivative 4 as a good intermediate by condensation of compound 3 with thiosemicarbazone in the presence of acetic acid as catalyst afforded compound 4. Physical properties and spectral data confirmed its structure as 2-(a1-(2-((4-fluorophenyl1)-amino)-4-methylthiazol-5-yl) ethylidene)hydrazine-1-carbothioamide.

The IR spectrum for hybrid 4 showed absorption band at 3436 cm^{-1} assignable for NH, and abroad peak related to primary amine (NH_2) at 3160 cm^{-1} as well as absorption band at 1625 cm^{-1} for (C=N), while its ^1H NMR spectra indicated presence of singlet peak at 10.31 ppm corresponding to 2H of NH_2 , two singlet signals at 9.11, 9.66 ppm related to 2H of 2NH and appearance of the *para* system at the aromatic region *δ* 7.16 -7.58 ppm which integrated for 4 protons, furthermore-its ^{13}C NMR

confirmed the presence of azomethine (C=N) and thione (C=S) carbons at 159.16, 182.30 ppm respectively in addition to aliphatic and aromatic carbons.

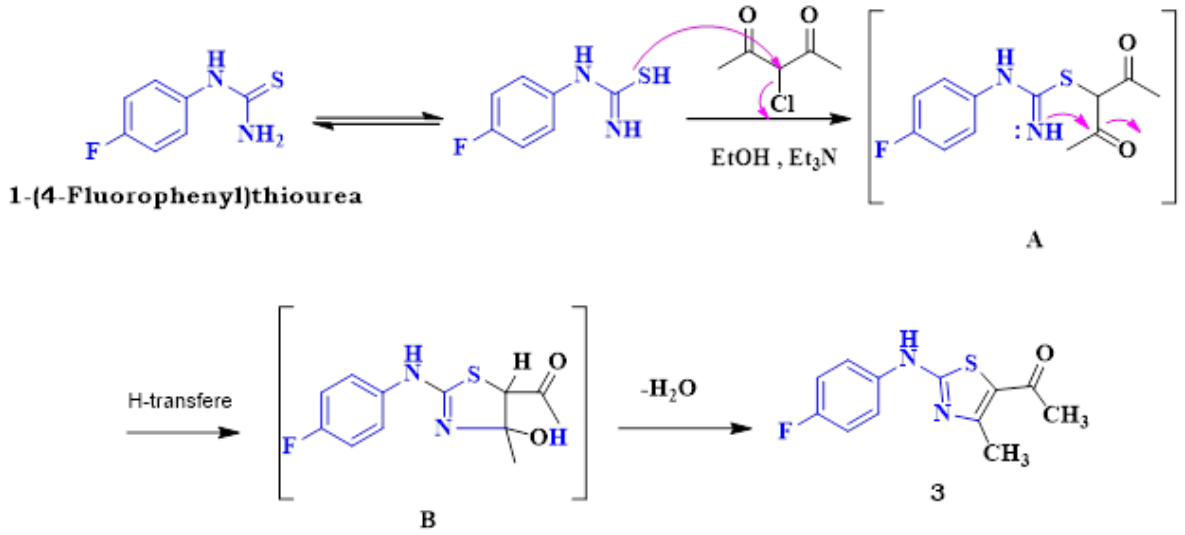

Scheme 2. Mechanism of the formation of a1-(2-((4-fluorophenyl) amino)-4-methyl thiazole-5-yl) ethan-1-one (3).

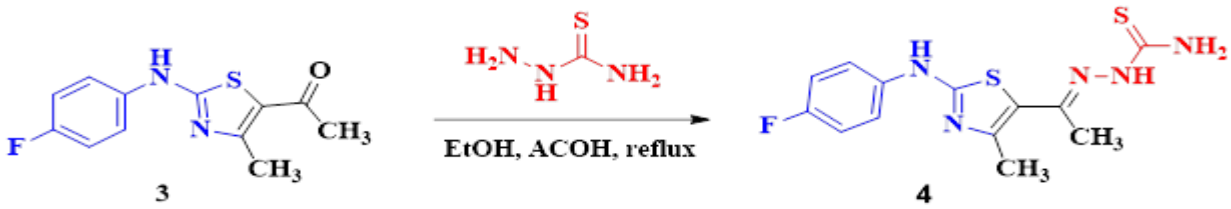

Scheme 3. Synthesis of 2-(1-(2-((4-fluorophenyl1)amino)-4-methylthiazol-5-yl)ethylidene)-hydrazine-1-carbothioamide (4)

We use compound 4 as a key starting material for alkylation with phenacyl bromide derivatives to produce *bis*-thiazole derivatives by refluxing in ethanol catalyzed by triethyl amine. Thin-layer chromatography (TLC) follow-up of the crude product[44] confirmed that compounds 6–8 were obtained in each case from our synthetic pathway. Based on their spectral data, the structure of the isolated products 6–8 was clarified. Compounds 6–8 have IR spectra with absorption bands at υ (3328-3200) and (1613–1606) cm^{-1}, corresponding to NH and C=N groups, respectively. The ^{1}H NMR for compound 6 showed the presence of singlet signal at δ 7.15 ppm related to thiazole-H at position 5, the aromatic protons appeared as *para* system, exhibited for 8 protons at δ 7.10 (J = 9.0 Hz), 7.19 (J = 9.0 Hz), 7.60 (J = 9.0 Hz), 7.83 (J = 8.0 Hz), and two singlet signals. at δ 10.24, 11.13 ppm related to the 2NH protons beside two singlet signals at δ 2.27, 2.41 ppm corresponding to $2CH_3$.While the ^{1}H NMR spectrum of acompound 7 revealed two singlet signals at δ 10.30, 11.46 ppm, related to the 2NH protons. and the aromatic signals for 2 phenyl rings appeared as para system, integrated for 8 protons. the mass spectrum demonstrated a molecular ion peak at *m/z*: 457.82 (M^{+}, 23.70%), 459.22 (M^{+2}, 9.02%), corresponding to $C_{21}H_{17}ClFN_5S_2$ with a base peak at *m/z* 142.89. The structure of 8 was assigned upon compatible elemental analyses and spectral data, the IR spectrum has an additional broad absorption band at 3250 cm^{-1} corresponding to the OH group. Its ^{1}H NMR spectrum revealed the presence of three singlet signals at δ 9.63, 10.22, and 11.31 ppm corresponding to 2NH and OH protons respectively which confirm its structure, in addition to ^{13}C NMR spectrum showed signals at δ 154.03, 161.66 ppm related to (C=N) and (C-OH) respectively beside aliphatic and aromatic carbons.

3.2. Biology

3.2.1. Alpha Amylase, α-glucosidase Inhibition Activity, and Peroxisome Proliferator Activated Receptor γ [PPAR-γ] Agonist Activity

Changes in α-amylase activity impact how well carbohydrates are used as an energy source. For humans to properly break down complex carbs, this enzyme is essential. Targeting the inhibition of α-amylase is thought to be beneficial in treating conditions like diabetes, obesity, periodontal disorders, and dental cavities that are associated with the absorption of carbohydrates. Compound 7 demonstrated a hypoglycemic impact and was tested for its ability to inhibit α-amylase using acarbose as a positive control (IC_{50} = 0.108± 5 µg/mL)

Analogue 7 had weak α-amylase inhibitory potential which represented IC_{50} value 84.4± 4.19µg/mL, contrasted with the usual medication acarbose, which was shown to be 0.108± 0.005 µg/mL (Table 1).

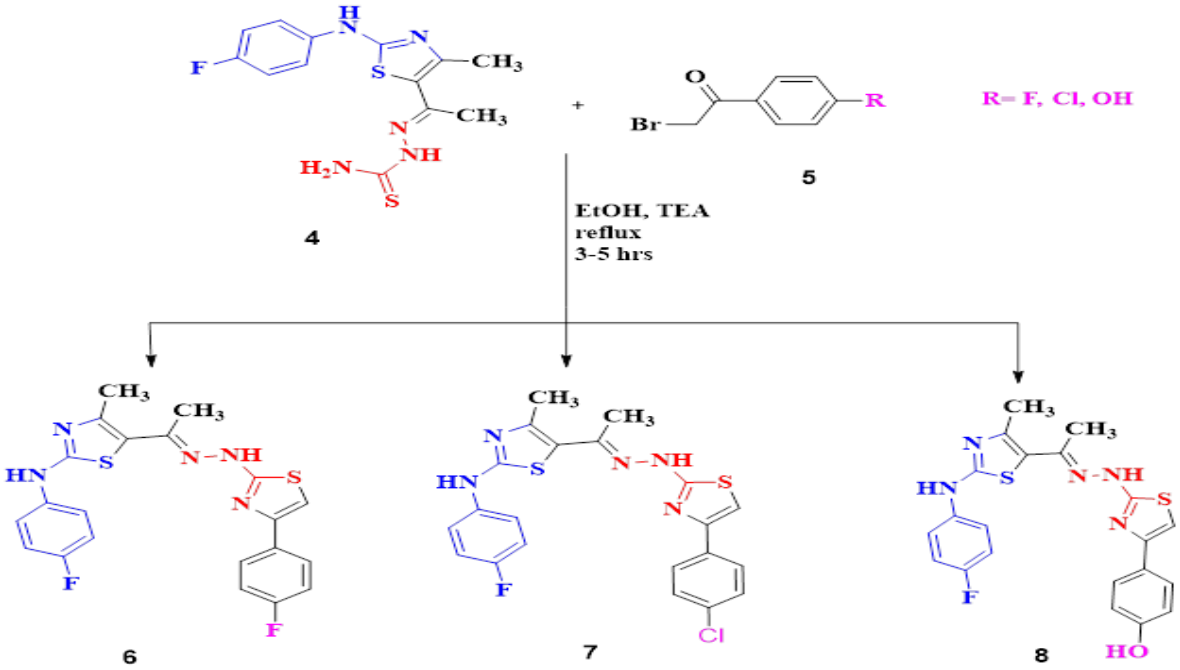

Scheme 4. Synthesis of bis- thiazole derivatives 6-8.

The brush border of the small intestine is home to the enzyme α-glucosidase, which catalyzes the enzymatic hydrolysis of 1,4-linked polysaccharides and yields glucose as one of the principal byproducts. Because glucose serves as one of the main sources of energy for eukaryotes, it is important to target α-glucosidase for the regulation of postprandial hyperglycemia. Acarbose and other anti-diabetic drugs known as α-glucosidase Inhibitors (AGIs) function by preventing the gastrointestinal system from absorbing glucose[45]. Using the kit technique, the IC_{50} value of Acarbose's inhibition of α-glucosidase activity was determined to be 0.74 ± 0.15 mM/mL. Table **1** shows that compound 7 exhibited a good inhibitory effect on α-glucosidase, with IC_{50} value of 3.708±0.07 mM/mL. As a member of a broad family of nuclear hormone receptors that are activated by ligands, PPAR-γ is a crucial target for medications that control glucose metabolism. Insulin sensitivity is raised in adipose, muscle, and hepatic tissues by PPAR-γ. There are two primary kinds of PPAR-γ: PPAR-γ1, which is present in all tissues except muscles, and PPAR-γ2, which is found in the intestine and adipose tissues. Using the human PPAR-γ (Peroxisome Proliferator Activated Receptor Gamma) ELISA Kit Catalogue No. MBS2503174, hybrid 7 was further assessed to determine its *in vitro* PPAR-γ binding affinity. 1.912±0.11 ng/mL was the IC_{50} value of pioglitazone, which was utilized as a positive control. As demonstrated in Table **1**, compound seven had a greater affinity for PPAR-γ than pioglitazone, with IC_{50} value of 1.057±0.030 ng/ML higher than that of pioglitazone.

3.2.2. Test for Blood Glucose Levels.

The results of the blood glucose level test are shown in

Table . All the tested compounds have shown good activity in the reduction of blood glucose level as compared with normal control rats, one tested compound 7 out of three namely 6, 7, 8 had showed significant reduction in blood glucose level, more efficient than pioglitazone, a standard drug used.

Table 1. The percent inhibition (IC_{50}) of α- Amylase, α-glucosidase and PPAR-γ activation by compound 7.

Seria.	**Cpds. No.**	**IC_{50} α- Amylase (µg/mL)**	DF=10± SD
1	7	84.4	4.19
2	**Acarbose**	**0.108**	0.005
		IC_{50} α-Glucosidase (mM/mL)	DF=100± SD
1	7	3.708	0.07
2	Acarbose	0.74	0.15
PPAR-γ (ng/mL)			
1	7	1.057±0.030	
2	Pioglotazone	1.912±0.11	

Table 2. Target compound's effects on blood glucose levels.

NO.	**Group**	**Fasting Blood Glucose Level mg/dL**	**After 0.5 hours, blood glucose level in mg/dL.**	**After 1 hour, blood glucose level in mg/dL.**
Group 1	Cont.	71.67±3.528	129.00±2.082	125.30±1.453
Group 2	Pioglitazone	71.33±1.856	127.00±4.359	94.67±5.783 [a]
Group 3	6	71.00±3.786	127.70±3.480	106.70±5.207
Group 4	7	72.00±4.359	132.70±4.256	90.67±5.239 [a]
Group 5	8	77.00±4.359	134.30±2.728	137.30±10.40

For each treatment, each value indicates the mean ± S.E.M. n = 6.
Shows the statistical significance in relation to the control after one hour ($P < 0.05$).

3.3. *In silico* Investigations

3.3.1. Physicochemical and ADME Characteristics Investigated in Silico

Along with the common reference medications acarbose and pioglitazone, compound **7** was subjected to drug likeliness, pharmacokinetic/ADME, and physicochemical *in-silico* calculations. These included, among other physical parameters, molar refractivity, water solubility, number of rotatable bonds, atomic class count, and lipophilicity. One effective physiochemical pathway for affecting medication distribution is the TPSA. Using the stated equation (ABS = 109 − (0.345 × TPSA) [46,47], the absorption rate of compound **7** was computed. From a physicochemical perspective, there were no violations of Lipinski's requirements for oral medications. This behavior is like that of pioglitazone, but it is better than Acarbose, which showed three breaches of Lipinski's **Table 3**. It had also shown no evidence of Veber's infractions. In addition, the presence of six rotatable bonds suggests that it possessed a comparable level of molecular-flexibility to the biological targets of acarbose and pioglitazone, which have nine, and seven rotatable bonds, respectively.

It has been demonstrated that the topological polar surface areas (TPSA) of all active chemicals are less than 200 Å2. Additionally, the formula % ABS = 109 – (0.345 x TPSA) 41,42 was used to calculate the absorption (percent ABS). Compound **7**'s calculated ABS percent is 68.06 percent, close to pioglitazone's but much higher than that of acarbose. This indicates that, even if **Table 3** of the biological activity discussion section shows that this chemical has a potential effect against α-amylase and α-glucosidase, it may have a cell-membrane permeability and bioavailability that focuses its action more on PPAR-γ activation.

Pharmacokinetic and medicinal chemistry data revealed that compound **7** had no passive blood-brain barrier permeability, like acarbose, and low GI absorption similar to acarbose and pioglitazone. It does not thus have any CNS side effects. P-glycoprotein's (P-gp) non-substrate candidature is another noteworthy characteristic. As an efflux transporter, P-gp removes medications, other chemicals, and their substrate from cells. as

illustrated in **Table 4**. The P-gp protein was demonstrated to not bind to compound **7**. It is comparable to pioglitazone and better than acarbose due to its very low propensity to efflux out of the cell and has a maximal effect.

The most important factor influencing absorption is a drug's bioavailability, which is a measurement of the drug's concentration in the bloodstream. It's interesting to note that its bioavailability is good, with values of 0.55 that are superior to acarbose and on par with pioglitazone. SwissADME's Pan Assay Interference Compounds (PAINS) could not detect any hit alerts. PAINS are crucial factors to consider while creating drugs to reduce false-positive results; yet, if these filters are overvalued or used without proper judgement, it can result in prospective accomplishments being rejected because of phantom PAINS[48]. Compound **7** has a synthetic accessibility of 3.69, which indicates that it may be produced synthetically in large numbers, just like pioglitazone **Table 4**.

In this case, **Figure 2**, the sp3 carbons fraction in all compounds is less than 0.25.

Table 3. The number of rotatable-bonds and the physicochemical parameters based on Lipinski's rule of five in addition to Physicochemical properties based on TPSA and % ABS

Cpd. No.	HBD< 5	HBA< 10	MlogP< 4.15	MW< 500	Lipinskis´ Violations	Vebers´ violation	Rotatable Bonds
7	2	4	3.97	457.97	0	0	6
Acarbose	14	19	-6.94	645.6	3	1	9
Pioglitazine	1	4	2.01	356.44	0	0	7

Cpd. no.	TPSA	% ABS
7	118.68	68.06
Acarbose	321.17	-1.80
Pioglitazine	93.59	76.71

Table 4. Characteristics of medicinal chemistry and pharmacokinetics

Cpds. No.	GI. Absorption	BBB. Permeation	Pg. Substrate	Bioavailability Score	PAINS Alerts	Synthetic Accessibility
7	Low	No	No	0.55	0	3.69
Acarbose	Low	No	Yes	0.17	0	7.34
Pioglitazine	High	No	No	0.55	0	3.46

3.4. Toxicity studies

As represented in **Error! Reference source n ot found.**, the following web tools were used to analyse the toxicity of chemical 7 and two FDA-approved antidiabetic medications, pioglitazone and acarbose: AProTox-II (https://tox-new.charite.de/protox_II) and apkCSM (http://biosig.unimelb.edu.au/pkcsm/prediction) [44, 45, 49, 50].

According to the pkCSM web tools, hybrid 7 has no AMES toxicity, unlike Acarbose and Pioglitazone. Compound 7 exhibited Oral Rat Acute Toxicity (LD_{50}) values of 2.92, which were equivalent to those of anacarbose and apioglitazone (2.449 and 2.258 mol/kg, respectively). However, the Oral Rat Chronic Toxicity values have been determined to be 0.498 log mg/kg.bw/day). This medication is regularly withdrawn from theclinical studies and theproduction due to hepatotoxicity.Liver slices, immortalised cell lines like HepG-2, or primary human hepatocyte cultures can all be used in in vitro experiments. The toxicity endpoint was examined using the pkCSM server. In addition to Pioglitazone, compound 7 was tested and expected to be hepatotoxic; however, there was no evidence of skin sensitivity.

Table 5. Toxicity of the most active compound 7 as well as Acarbose and Pioglitazone

Test Compound	**The most active compound 7**		
	pkCSM		
	7	Acarbose	Pioglitazone
AMES toxicity	No	No	No
Max. tolerated dose (human)	0.406	0.435	0.41
hERG I inhibitor	No	No	No
hERG II inhibitor	Yes	Yes	No
Oral Rat Acute Toxicity (LD_{50})	2.92	2.449	2.258
Oral Rat Chronic Toxicity (LOAEL)	0.498	5.319	1.379
Hepatotoxicity	Yes	No	Yes
Skin Sensitization	No	No	No
T.Pyriformis toxicity	0.319	0.285	1.138
Minnow toxicity	-0.765	16.823	0.094
ProTox-II prediction			
LD_{50} (mg/kg)	1000	24000	1000
Toxicity Class	IV	VI	IV
Immunotoxicity	Inactive 0.94	Active 0.99	Inactive 0.89
Mutagenicity	Inactive 0.50	Inactive 0.76	Inactive 0.71
Cytotoxicity	Inactive 0.80	Inactive 0.70	Inactive 0.73
Phosphoprotein (Tumor Suppressor) p53	Inactive 0.86	Inactive 0.97	Inactive 0.91

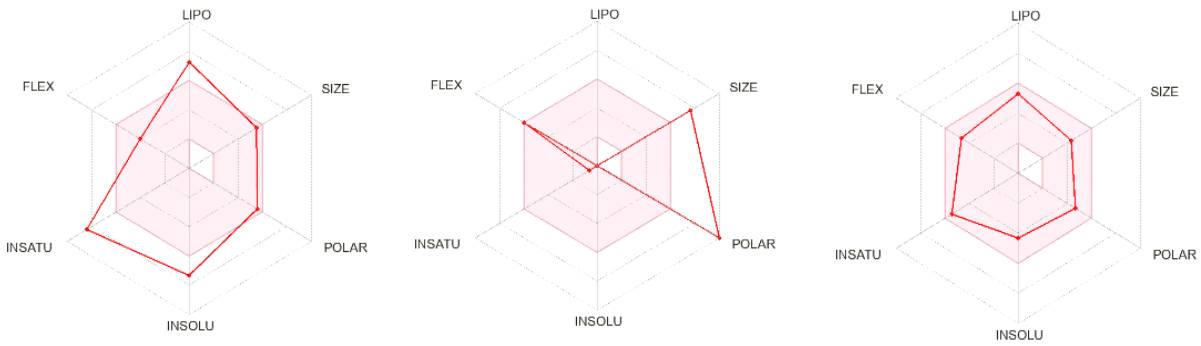

7 **Acarbose** **Pioglitazone**

Figure 2. The studied substances' bioavailability radar in comparison to acarbose and pioglitazone.

ProTox-II detection predicted that Acarbose would belong in class six (GHS) of the global harmonized system of a chemical labelling categorization, while compound 7 and a pioglitazone would belong in class four Table 5. It was expected that Compound 7 would neither be immunotoxic, in contrast to acarbose, nor cytotoxic or mutagenic, in contrast to acarbose and pioglitazone. Additionally, it was anticipated that chemical 7 would not exhibit any harmful effects. Compound 7 had an LD_{50} value of 1000 mg/kg, which is equivalent to pioglitazone.

Table 6. Binding energies S (Kcal mol−1), receptor interactions and distances in angstroms of Acarbose and Pioglitazone (London dG as scoring function).

Ligand/ Protein	Binding Energy (*S*) (kCal/mol)	Receptor Amino Acid names and number	Type of interaction	Distance (Å)
Acarbose/ *α*-amylase	-9.54	GLU240	H-donor	2.78
		HIS 201	H-donor	2.67
		GLU233	H-donor	2.58
		GLU233	H-donor	2.63
		ASP 300	H-donor	3.03
		GLU233	H-donor	3.26
		ASP 300	H-donor	2.54
		ASP 197	H-donor	3.37
		ASP 197	H-donor	2.7
		ASP 300	H-donor	3.18
		TRP 59	H-donor	2.69
		THR 163	H-donor	2.8
		LYS 200	H-acceptor	2.77
		ARG 195	H-acceptor	2.91
		HIS 299	H-acceptor	3.06
		HIS 299	H-acceptor	3.37
		HIS 305	H-acceptor	2.76
		GLN63	H-acceptor	2.86
		TYR 151	H-pi	4.59
		TRP 59	H-pi	4.47
		TRP 59	H-pi	3.92
Acarbose/ *α*-glucosidase	-19.54	ASP 282	H-donor	2.77
		ASP 282	H-donor	2.65
		MET 519	H-donor	3.18
		ASP 616	H-donor	3.24
		MET 519	H-donor	4.32
		ASP 616	H-donor	2.55
		ASP 404	H-donor	2.65
		ASP 404	H-donor	2.54
		ARG 600	H-acceptor	2.64
		HIS 674	H-acceptor	2.87
		PHE 649	H-pi	4.28
Pioglitazone/ PPAR-*γ*	-12.77	MET 364	H-donor	3.68
		MET 348	H-donor	4.07
		SER 289	H-acceptor	2.63
		HIS 323	H-acceptor	2.76
		TYR 473	H-acceptor	2.8
		HIS 449	H-acceptor	2.91
		CYS 285	pi-H	3.82

3.5. Docking Studies

Twelve H-bond donors and six H-bond acceptors interact with *α*-amylase through the natural ligand Acarbose, including Glu240, His201, Glu233, Asp300, Asp197, Trp59, and Thr163. Moreover, Tyr151 and Trp59 amino acids are involved in three H-arene interactions. An overview of the interactions can be seen in Table 6. The amino acids with which acarbose interacts with *α*-glucosidase are Arg600 and His674, two H-bond acceptors, Asp282, Asp616, Asp404, and Met519, eight H-bond donors, and one H-arene interaction, Phe649. Pioglitazone interacts with PPAR-*γ* *via* two H-bond donors (Met364 and Met348), one arene-H interaction (Cys285), four H-bond acceptors (Ser289, His323, Tyr473 and

His449), and one arene-H interaction. An overview of the interactions can be seen in Table 6.

In case of PPAR-*y*, compound 7 was docked, and exhibited binding energy scores values of -14.30 and showed three interactions with the binding pocket, which include three arene-H interactions with Cys 285, Ile 341, and Ser 342. Interactions are summarized in **Error! Reference source not found.**.

Table 7 shows the binding modalities of each chemical with aPPAR-*y*.

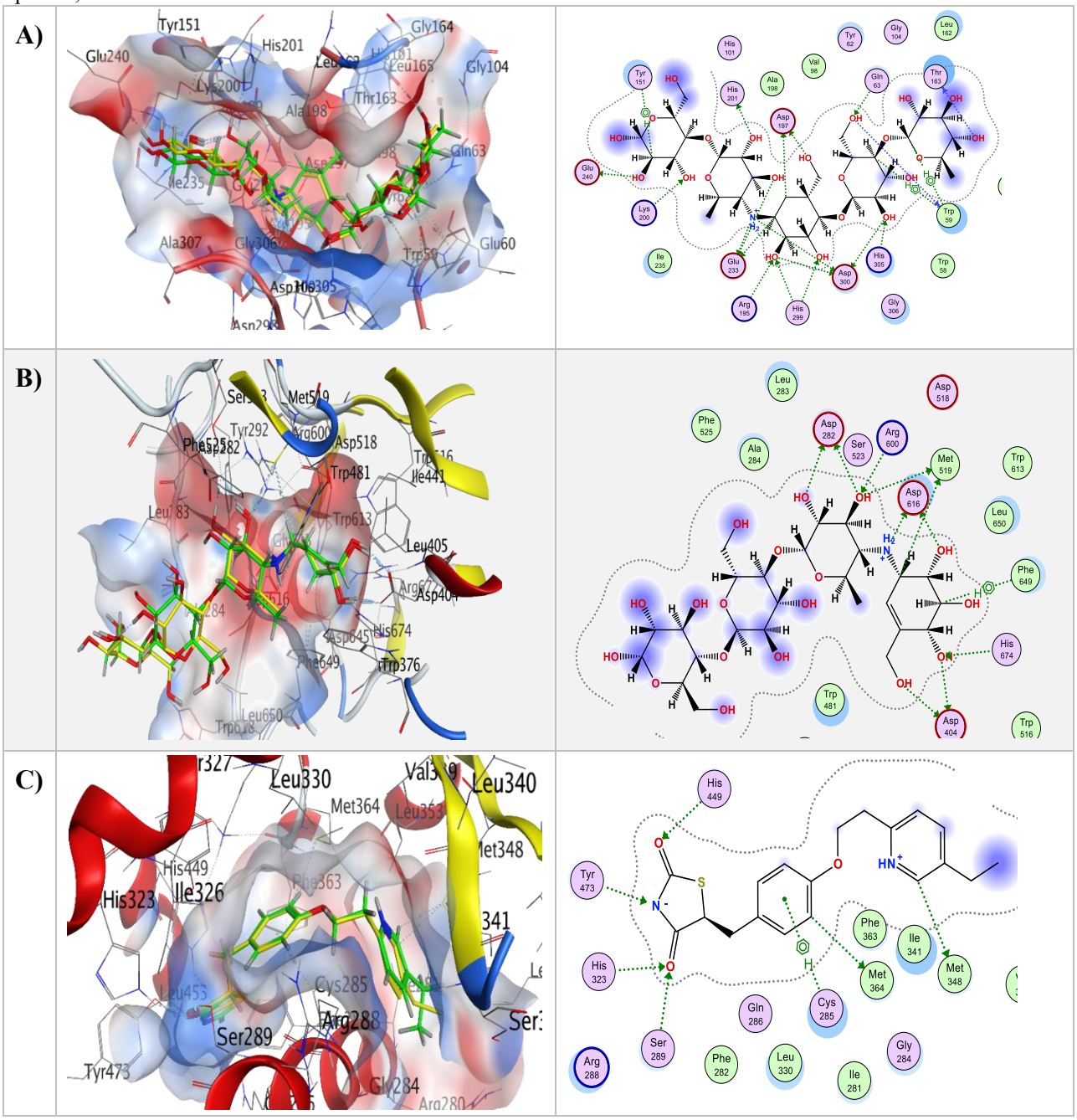

Figure 3. A) 2D interactions and overlay of acarbose in α-amylase (PDB ID: 1B2Y) (RMSD= 0.6385 Å) with co-crystallized ligand (yellow) and re-docked pose (green). B) Two-dimensional interactions and overlay between the re-docked posture (green) and co-crystallized ligand (yellow) of Acarbose in α-glucosidase (PDB ID: 5NN8) (RMSD= 0.5693 Å). C) Two-dimensional interactions and overlay between the re-docked posture (green) and co-crystallized ligand (yellow) of pioglitazone (RMSD= 0.3703Å).

Table 7. Binding energies S (kCal mol^{-1}), receptor interactions and distances in angstroms of Compounds 7 (London dG as scoring function) with PPAR-*ɣ* (PDB ID: 5Y2O) in addition to Binding mode as well as 2D interactions of the pocket of PPAR-*ɣ* (PDB ID: 5Y2O) with Compound 7.

Compound	Binding Energy (*S*) (kCal/mol)	Receptor Amino Acid	Type of interaction	Distance (Å)
		5Y2O		
7	-14.30	CYS 285	pi-H	4.16
		ILE 341	pi-H	3.96
		SER 342	pi-H	4.19

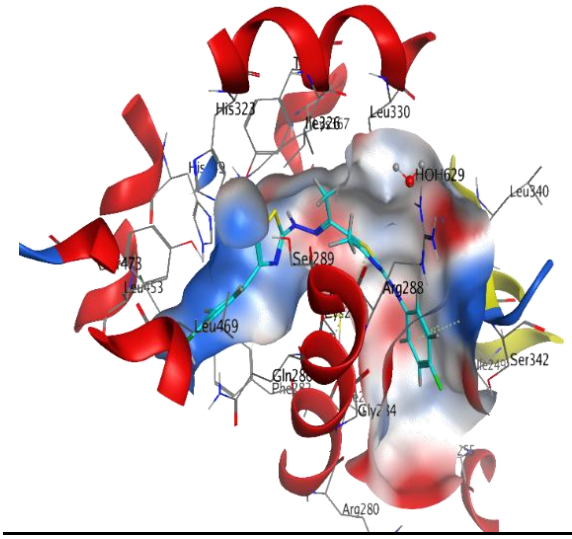

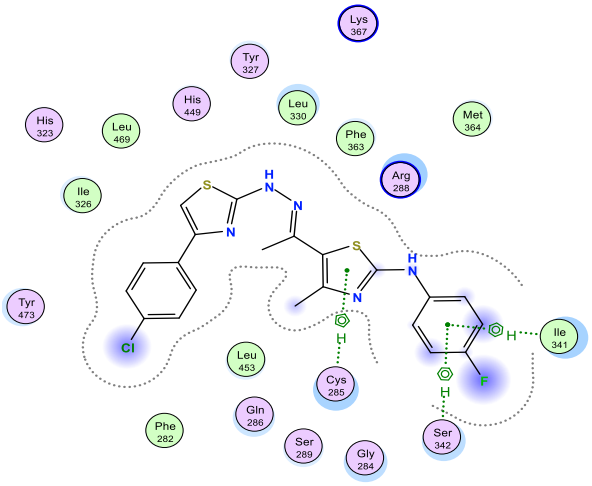

5. CONCLUSIONS

Bis-thiazole derivatives **6-8** have been synthesized and evaluated *in vivo* for their hypoglycemic effect, plus *in vitro* evaluation for enzymes involved in carbohydrates metabolism and glucose uptake, including alpha-amylase, alpha-glucosidase inhibitory potential, in addition to PPAR gamma agonist activity. One out of three derivatives displayed significant PPAR gamma agonist activity with an IC_{50} value of 1.057±0.030 ng/mL, surpassing the IC_{50} value of pioglitazone (1.912 ± 0.11 ng/mL), while the same compound showed good alpha-amylase inhibitory activity with an IC_{50} value of 3.708± 0.07 mM/mL. Using a molecular docking analysis, the binding relationship of analogues with protein ligands' active sites was verified.

Funding: No funding

Conflicts of Interest: The authors declare no conflict of interest.

Ethical Statement: The research was conducted in adherence to the ethical guidelines set by the Faculty of Pharmacy at Al-Azhar University, Egypt ethical approval number (405). The handling of the animals followed the guidelines outlined in the publication titled "Guide for Care and Use of Laboratory Animals" (NIH Publication No. 85-23, revised 2011).

Author Contribution: Conceptualization, E.A.F., Y.A.A., H.M.A.E., and M.S.A.; Data curation, A.T.M., E.A.F., Y.A.A., H.M.A.E., and M.S.A.; Formal analysis, A.T.M., E.A.F., H.M.A.E., S.M.A., and M.S.A.; Investigation, A.T.M., E.A.F., Y.A.A. and M.S.A.; Methodology, A.T.M., E.A.F., H.M.A.E., and M.S.A.; Project administration, E.A.F., and Y.A.A.; Resources, E.A.F., A.T.M.; Software, E.A.F.; Supervision, E.A.F., Y.A.A. and S.M.A.; Validation, E.A.F., S.M.A., and H.M.A.E.; Writing—original draft, E.A.F., A.T.M., H.M.A.E., and M.S.A.; Writing—review & editing, E.A.F., A.T.M., S.M.A., and M.S.A.

List of Abbreviations: PPAR-γ: Peroxisome proliferator-activated Receptor, TZD: Thiazolidinediones, TSCs: Thiosemicarbazones, TPSA: Topological Polar Surface Area.

REFERENCES

1. Agarwal.P, Gupta.R, Alpha-amylase inhibition can treat diabetes mellitus, Res. Rev. J. Med. Heal. Sci. 5 (2016) 1–8.
2. American Diabetes Association. Diagnosis and classification of diabetes mellitus. Diabetes Care. 2009 Jan;32 Suppl 1(Suppl

1):S62-7. https://doi.org/10.2337/dc09-S062

3. Adeghate. E, Schattner.P, Dunn.E, An update on the etiology and epidemiology of diabetes mellitus, Ann. N. Y. Acad. Sci. 1084 (2006) 1–29. https://doi.org/10.1196/annals.1372.029
4. Cheekurthy.A,.J Ramb,abu. C, Kumar. A, Prevalence of Type 2 Diabetes Mellitus among Women and the Associated Risk Factors, Research & Reviews: Journal of Nursing & Health Sciences, RRJNHS, Volume 2, Issue 2 (2016) 26–30.
5. Borde. R.M, Dhavse s. J. R, munde, a. S design, synthesis, and pharmacological evaluation of some novel bis-thiazole derivatives, Innovare Academic Sciences Pvt Ltd. DOI: http://dx.doi.org/10.22159/ajpcr.2018.v11i4.23413
6. Adeghate. E, Schattner. P, Dunn. E, An update on the etiology and epidemiology of diabetes mellitus, Ann. N. Y. Acad. Sci. 1084 (2006) 1–29. https://doi.org/10.1196/annals.1372.029
7. Kothari. M, Kannan. K Sahadevan. R, Sadhukhan. S, Novel molecular hybrids of EGCG and quinoxaline: Potent multi-targeting antidiabetic agents that inhibit α-glucosidase, α-amylase, and oxidative stress,International Journal of Biological Macromolecules 263 (2024) 13017, https://doi.org/10.1016/j.ijbiomac.2024.130175
8. Li. J, Lian. H, Recent development of single preparations and fixed-dose combination tablets for the treatment of non-insulin-dependent diabetes mellitus: A comprehensive summary for antidiabetic drugs, Arch. Pharm. Res. 39 (2016) 731–746. https://doi.org/10.1007/s12272-016-0762-4
9. Vardanyan R, Hruby V. Synthesis of best-seller drugs. Academic press; 2016 Hyperglycemic and Hypoglycemic Drugs, https://doi.org/10.1016/B978-0-12-411492-0.00026-2
10. Monsalve.F.A,Pyarasani.R.D., Delgado-lopez. F,Moore-carrasco. R, Peroxisome Proliferator-Activated Receptor Targets for the Treatment of Metabolic Diseases, Hindawi Publishing Corporation, Volume 2013, Article ID 549627, 18 pages http://dx.doi.org/10.1155/2013/549627
11. Rahim. F, Tariq. S, Taha.M, Ullah.H, Zaman.K, Uddin. I, Wadood.A, Khan. A.A, Rehman. A.U, Uddin.N, Zafar. S, Shah .S.A.A., New triazinoindole bearing thiazole/oxazole analogues: Synthesis, α-amylase inhibitory potential and molecular docking study, Bioorg. Chem. 92 (2019) 103284. https://doi.org/10.1016/j.bioorg.2019.103284
12. Martin A.E., Montgomery P.A., Acarbose: An a-glucosidase inhibitor, Am J Health-Syst Pharm 53 (1996) 2277–2290.
13. Alva.M.L., Gray A., Mihaylova B., Leal J., Holman R.R., The impact of diabetes-related complications on healthcare costs: New results from the UKPDS (UKPDS 84), Diabet. Med. 32 (2015) 459–466. https://doi.org/10.1111/dme.12647
14. Singh N.Sharma U.S, Sutar N., Kumar S.Sharma U.K,Synthesisand antimicrobial activity of some novel 2-amino thiazole derivatives, J. Chem. Pharm. Res., 2010, 2(3)691-698.
15. Nanjan M.J., Mohammed M., Kumar B.R.P., Chandrasekar M.J.N., Thiazolidinediones as antidiabetic agents: A critical review, Bioorg. Chem. (2018). https://doi.org/10.1016/j.bioorg.2018.02.009
16. Nayak S, Gaonkar S.L., A Review on Recent Synthetic Strategies and Pharmacological Importance of 1 , 3-Thiazole Derivatives, Mini Reviews in Medicinal Chemistry 19 (2019). https://doi.org/10.2174/1389557518666180816112151
17. Dawood K.M., Raslan M. A., Abbas A. A., Mohamed B. E., Abdellattif M. H., Nafie M. S. and Hassan M. K., Novel Bis-Thiazole Derivatives: Synthesis and Potential Cytotoxic Activity Through

Apoptosis With Molecular Docking Approaches, frontiers in chemistry doi: 10.3389/fchem.2021.694870

18. Heffeter P., Pape V.F.S., Enyedy É.A., Keppler B.K., Szakacs G., Kowol C.R., Anticancer thiosemicarbazones: Chemical properties, interaction with iron metabolism, and resistance development, Antioxidants and Redox Signal. 30 (2019) 1062–1082. https://doi.org/10.1089/ars.2017.7487
19. Li.J, Lian.H, Recent development of single preparations and fixed-dose combination tablets for the treatment of non-insulin-dependent diabetes mellitus: A comprehensive summary for antidiabetic drugs, Arch. Pharm. Res. 39 (2016) 731–746. https://doi.org/10.1007/s12272-016-0762-4
20. Govindan, J., & Evans, M. (2012). Pioglitazone in Diabetes Ther. 3, 1-8.https://doi.org/10.1007/s13300-012-0001-z
21. Nazreen. S, Alam M.S., Hamid. H, Yar. M.S., Shafi. S, Dhulap. A, Alam. P, Pasha M.A.Q., Bano. S, Alam M.M., Haider. S, Ali. Y, Kharbanda. C, Pillai K.K, Design , synthesis , in silico molecular docking and biological evaluation of novel oxadiazole based thiazolidine-2 , 4-diones bis -heterocycles as PPAR- g agonists, 87 (2014) 175–185. https://doi.org/10.1016/j.ejmech.2014.09.010
22. Solangi M, Kanwal, K.M. Khan, S.Chigurupati, Saleem. F, Qureshi. U, Ul-Haq .Z, Jabeen, Felemban S.G. , Zafar. F, Perveen. S, Taha. M, Bhatia. S, Isatin thiazoles as antidiabetic : Synthesis , in vitro enzyme inhibitory activities , kinetics , and in silico studies, Arch. Pharm. (2022) 1–15. https://doi.org/10.1002/ardp.202100481
23. Omar A.M., Bajorath. J, Ihmaid. S, Mohamed. H.M., El-Agrody A.M., Mora . A, El-Araby. M.E. , Ahmed H.E.A. , Novel molecular discovery of promising amidine-based thiazole analogues as potent dual Matrix Metalloproteinase-2 and 9 inhibitors: Anticancer activity data with prominent cell cycle arrest and DNA fragmentation analysis effects, Bioorg. Chem. 101 (2020) 103992. https://doi.org/10.1016/j.bioorg.2020.103992
24. Iqbal A.K.M., Khan A.Y., Kalashetti M.B., Belavagi N.S., Gong. Y, Khazi I. A.M., Synthesis , hypoglycemic and hypolipidemic activities of novel thiazolidinedione derivatives containing thiazole / triazole / oxadiazole ring, Eur. J. Med. Chem. 53 (2012) 308–315. https://doi.org/10.1016/j.ejmech.2012.04.015
25. Tesfaye. A, Makonnen. E, Gedamu. S, Hypoglycemic and antihyperglycemic activity of aqueous extract of Justicia Schimperiana leaves in normal and streptozotocin-induced diabetic mice., Int. J. Pharma Sci. Res. (2016) 7(2), 110-113.
26. Kulkarni N. V., Revankar V.K., Kirasur B.N., Hugar M.H., Transition metal complexes of thiosemicarbazones with quinoxaline hub: An emphasis on antidiabetic property, Med. Chem. Res. 21 (2012) 663–671. https://doi.org/10.1007/s00044-011-9576-6
27. Perez-Gutierrez R.M. , Damian-Guzman M., Meliacinolin: A Potent α-Glucosidase and α-Amylase Inhibitor Isolated from Azadirachta indica Leaves and in Vivo Antidiabetic Property in Streptozotocin-Nicotinamide-Induced Type 2 Diabetes in Mice, Biol. Pharm. Bull. 35(9) 1516–1524(2012).
28. Daina. A, Michielin. O, and Zoete. V, "SwissADME: a free web tool to evaluate pharmacokinetics, drug-likeness and medicinal chemistry friendliness of small molecules," Scientific Reports, vol. 7, p. 42717, Mar 3 2017.
29. Fayed. E. A., Nosseir E. S. , Atef. A and El-Kalyoubi S. A. , "In vitro antimicrobial evaluation and in silico studies of coumarin derivatives tagged with pyrano-pyridine and pyrano-pyrimidine moieties as DNA gyrase inhibitors," Molecular Diversity, pp. 1-23, 2021.
30. Fayed E. A. , Bayoumi A. H. , Saleh A. S. , Al-Arab E. M. E. , and Ammar Y. A. , "In

vivo and in vitro anti-inflammatory, antipyretic and ulcerogenic activities of pyridone and chromenopyridone derivatives, physicochemical and pharmacokinetic studies," Bioorganic Chemistry, vol. 109, p. 104742, 2021.

31. Ammar.Y. A., Elhagali G. A., Abusaif.M.S, Selim. M.R, Zahran M. A. , Naser T. , et al., "Carboxamide appended quinoline moieties as potential anti-proliferative agents, apoptotic inducers and Pim-1 kinase inhibitors," Medicinal Chemistry Research, vol. 30, pp. 1649-1668, 2021.
32. Fayed E. A. , Al-Arab E. M. E. , Saleh A. S. , Bayoumi A. H. , and Ammar Y. A. , "Design, synthesis, in silico studies, in vivo and in vitro assessment of pyridones and thiazolidinones as anti-inflammatory, antipyretic and ulcerogenic hits," Journal of Molecular Structure, vol. 1260, p. 132839, 2022.
33. Fayed E. A. , Gohar N. A. , Farrag A. M. , and Ammar Y. A. , "Upregulation of BAX and caspase-3, as well as downregulation of Bcl-2 during treatment with indeno [1, 2-b] quinoxalin derivatives, mediated apoptosis in human cancer cells," Archiv der Pharmazie, vol. 355, p. 2100454, 2022.
34. .Roig-Zamboni. V, Cobucci-Ponzano. B, Iacono. R, Ferrara. M. C, Germany. S, Bourne. Y, Parenti.G, Moracci. M, Sulzenbacher. G, Structure of human lysosomal acid alpha-glucosidase-a guide for the treatment of Pompe disease., Nat Commun 2017, 8 (1), 1111.
35. Nahoum V. , Roux G. , Anton.V, Rougé P, Puigserver. A, Bischoff.H, Henrissat. B, Payan. F, Crystal structures of human pancreatic α-amylase in complex with carbohydrate and proteinaceous inhibitors, Biochem. J. 346 (2000) 201–208. https://doi.org/10.1042/0264-6021:3460201
36. .Lee.M. Tan A, L, Yang. H., Im.Y. G., Im.Y.J. , Structures of PPARgamma complexed with lobeglitazone and pioglitazone reveal key determinants for the recognition of antidiabetic drugs., Sci Rep 2017, 7 (1), 16837.
37. Molecular Operating Environment (MOE), 2014.09 Chemical Computing Group ULC, 1010 Sherbooke St. West, Suite #910, Montreal, QC, Canada,
38. Fayed.E. A., Thabet. A , Abd El-Gilil. Sh. M. , Elsanhory H. M.A., Ammar Y. A., Fluorinated thiazole–thiosemicarbazones hybrids as potential PPAR-γ agonist and α-amylase, α-glucosidase antagonists: Design, synthesis, in silico ADMET and docking studies and hypoglycemic evaluation, Journal of Molecular Structure, https://doi.org/10.1016/j.molstruc.2023.137374
39. Yan. Z, Liu. A, Ou. Y, Li .J, Yi.H, Zhang . N, Liu . M, Huang. L, Ren. J, Liu. W, Hu.A, Design , synthesis and fungicidal activity evaluation of novel pyrimidinamine moiety derivatives containing phenyl-thiazole / oxazole National Engineering Research Center for Agrochemicals , Hunan Research Institute Hunan Province Key Laboratory for Agroc, Bioorg. Med. Chem. (2019). https://doi.org/10.1016/j.bmc.2019.05.029
40. Mohinder. P, Harbinder. S.B., Sahil. S, CHEMISTRY Thiazole-5-carboxylic acid derivatives as potent xanthine oxidase inhibitors : design , synthesis , in vitro evaluation , and molecular modeling studies, Med. Chem. Res. (2019). https://doi.org/10.1007/s00044-019-02461-y
41. Santos. N,Junior. N, Oliveira. J, Duarte. D, Soares. J, Marques. D, Santos.A, .Nogueira.F ,.Pereira. V,. Lima. M, .Filho.I, Synthesis , characterization , antioxidant and antiparasitic activities new naphthyl-thiazole derivatives, Experimental Parasitology 248 (2023). https://doi.org/10.1016/j.exppara.2023.108498
42. de Oliveira. J.F., Lima. T.S., Vendramini-Costa. D.B, Pedrosa S.C.D.L., Lafayette. E.A, da Silva. R.M.F., de Almeida. S.M.V., Moura R.O.D., Ruiz A.L.T.G., de Carvalho. J.E. de Lima , M. d. C.A. , Thiosemicarbazones and 4-thiazolidinones indole-based derivatives: Synthesis, evaluation of antiproliferative activity, cell death mechanisms and

topoisomerase inhibition assay, Eur. J. Med. Chem. (2017),. https://doi.org/10.1016/j.ejmech.2017.05.023

43. Fayed. E.A., Ragab.A. , Ezz Eldin.R.R. , Bayoumi. A.H., Ammar.Y.A. , In vivo screening and toxicity studies of indolinone incorporated thiosemicarbazone, thiazole and piperidinosulfonyl moieties as anticonvulsant agents, Bioorg. Chem. 116 (2021) 105300. https://doi.org/10.1016/j.bioorg.2021.105300

44. Majeed. M., Majeed. S., Mundkur.L, Nagabhushanam.K, Arumugam. S, Beede.K, Ali. F, Standardized Emblica officinalis fruit extract inhibited the activities of α-amylase, α-glucosidase, and dipeptidyl peptidase-4 and displayed antioxidant po, J. Sci. Food Agric. (2020).100(2), 509-516. https://doi.org/10.1002/jsfa.10020

45. Nazreen.S, Alam M.S., Hamid. H., Shahar.M, Dhulap.A,Alam.P, Pasha.M. A. Q, Bano.S, Alam. M.M., Haider.S, Kharbanda.C, Ali. Y, Pillai.K.K., molecular docking, in vitro and in vivo antidiabetic activity with hepatotoxicity risk evaluation and effect on PPAR- $_{\gamma}$ gene expression, Bioorg. Med. Chem. Lett. 24 (2014) 3034–3042. https://doi.org/10.1016/j.bmcl.2014.05.034

46. Zhao.Y. H., Abraham.M. H., Le.J, Hersey.A, Luscombe C. N., Beck. G., et al., "Rate-limited steps of human oral absorption and QSAR studies," Pharmaceutical Research, vol. 19, pp. 1446-57, Oct 2002.

47. Fayed.E. A., Sabour. R, Harras.M. F., and Mehany A. B., "Design, synthesis, biological evaluation and molecular modeling of new coumarin derivatives as potent anticancer agents," Medicinal Chemistry Research, vol. 28, pp. 1284-1297, 2019.

48. Capuzzi S. J., Muratov E. N., and Tropsha.A, "Phantom PAINS: Problems with the Utility of Alerts for Pan-Assay INterference CompoundS," Journal of Chemical Information and Modeling, vol. 57, pp. 417-427, Mar 27 2017.

49. Pires D. E., Blundell.T. L., and Ascher. D. B. , "pkCSM: Predicting Small-Molecule Pharmacokinetic and Toxicity Properties Using Graph-Based Signatures," Journal of Medicinal Chemistry, vol. 58, pp. 4066-72, May 14 2015.

50. Banerjee.P, Eckert A. O., Schrey A. K., and Preissner.R., "ProTox-II: a webserver for the prediction of toxicity of chemicals," Nucleic Acids Research, vol. 46, pp. W257-W263, Jul 2 2018.